Use of Redundant Testing Functions in Moment-Method Solutions for Block Models

Salvatore Caorsi, Gian Luigi Gragnani, *Member, IEEE,* and Matteo Pastorino, *Member, IEEE*

***Abstract*— An overconstrained version of the method of moments for SAR evaluation in biological bodies is presented. A number of testing functions larger than the one of basis functions is used in order to better constrain the solution near corners and edges. A rectangular system is obtained that is solved by means of a pseudoinversion algorithm. Comparisons with results reported in the literature are made, showing an enhancement of the MoM capabilities in SAR calculations, without a consistent increase in computational requirements.**

I. Introduction

In THE past few years, the method of moments [1] has been proposed as an effective tool for evaluating the electric fields scattered by three-dimensional objects. In particular, it has been used to compute the distribution of electromagnetic energy inside biological bodies exposed to an incident electromagnetic field [2], [3]. The knowledge of the specific absorption rate (SAR) is necessary when one addresses dosimetry problems to prevent biohazards resulting from exposure to unwanted nonionizing radiation, or when one applies a medical therapy based on such a field (e.g., hyperthermia). More recently, to overcome the moment method's limitations (especially related to the expenses for computational resources), other methods have been devised. For example, the finite-element method and the finite-difference method have been proposed (for wide references, see, for example, [4]–[6]). The method of moments is currently widely employed, and the issue of its real capabilities is still being debated. In particular, pulse functions and block models have been discussed by many authors, sometimes of different opinions about the accuracy and effectiveness of such models. For example, Massoudi *et al.* showed that the convergence obtained by Livesay and Chen's method becomes doubtful when the number of cells increases [7]. Hagmann [8] proved that this can be avoided if the matrix elements are correctly computed and the discretization cells suitably fit the object boundary. Actually, the application of subsectional "hat" basis functions and point matching appears quite an efficient solution, in that, besides allowing very simple implementations, it offers a wide range of possibilities for modeling biological bodies, through the use of a reduced number of unknowns [9]. For the sake of completeness, however, it should be noted that more sophisticated (and more expensive in terms of computational resources) versions of the moment method for inhomogeneous dielectric objects were proposed by Schaubert *et al.* [10] and by Tsai *et al.* [11]. Up to now, many studies have been carried out on the use of suitable subsections and of the related basis functions. Instead, the aspects related to the implementation of the moment method on the basis of testing functions need to be further investigated, even though interesting considerations about the use of testing functions in the moment can already be found in [12] and in references therein cited.

In this paper, we aim to assess the moment method's capabilities by considering an overconstrained implementation [13]. We compare the results obtained in applying this method to simple test scatterers with the results reached by using the "classic" moment method [14]. The overconstrained version of the moment method (OMoM) employs a number of testing functions that is larger than the one of basis functions. We use pulse basis functions and Dirac's deltas as weighting functions. It is beyond the scope of this paper to discuss the accuracy of such basis and testing functions. The OMoM could also be implemented by means of different kinds of functions.

The proposed version of the moment method produces a rectangular linear system of algebraic equations, and a generalized inverse solution can be reached by applying a suitable algorithm [15], [16]. In the following, we summarize the theory of the method, and discuss some numerical results that show the possibility of evaluating the average electromagnetic energy deposition inside dielectric objects with higher accuracy, though by using a reduced amount of computer resources.

II. Overconstrained Version of the Moment Method

Let V be the space volume occupied by an inhomogeneous body illuminated by an incident electric field $\boldsymbol{E}_{\mathrm{inc}}(\boldsymbol{r})$. The total electric field at each point inside the body can be obtained—as is well known—by solving the equation:

$$\boldsymbol{E}(\boldsymbol{r}) = \boldsymbol{E}_{\mathrm{inc}}(\boldsymbol{r}) + \int_V \tau(\boldsymbol{r}')\boldsymbol{E}(\boldsymbol{r}')\boldsymbol{G}(\boldsymbol{r}/\boldsymbol{r}')\,d\boldsymbol{r}' \qquad (1)$$

where $\boldsymbol{G}(\boldsymbol{r}/\boldsymbol{r}')$ stands for Green's dyadic function for free space, and the function $\tau(\boldsymbol{r})$ is given by $\tau(\boldsymbol{r}) = \sigma(\boldsymbol{r}) - j\omega\varepsilon_0[\varepsilon_r(\boldsymbol{r}) - 1]$.

A moment-method solution of this equation can be obtained by expanding the unknown total electric field into a sum of N basis functions, $\boldsymbol{E}_1(\boldsymbol{r}), \cdots, \boldsymbol{E}_N(\boldsymbol{r})$:

$$\boldsymbol{E}(\boldsymbol{r}) = \sum_{n=1}^{N} \boldsymbol{E}_n(\boldsymbol{r}). \qquad (2)$$

If pulse basis functions are used, this implies the subdivision of the volume V into N subdomains V_n. We could use M_p testing

Manuscript received May 22, 1991; revised June 11, 1992.

The authors are with the Department of Biophysical and Electronic Engineering, University of Genoa, Via Opera Pia 11A, 16 145 Genoa, Italy.

IEEE Log Number 9204488.

functions for each pth value, $p = 1, \cdots, N$. If Dirac's deltas are used as testing functions, this is equivalent to considering M_p testing points for each subvolume. Substituting (2) into (1) and weighting the resulting equation by means of an inner product, we obtain an algebraic system of linear equations that can be written as

$$[G][E] = [E_i]. \tag{3}$$

The dimensions of the quantities involved in relation (3) are the following:

$$[E]: N \times 1 \tag{4}$$

$$[E_i]: \sum_{p=1}^{N} M_p \times 1 \tag{5}$$

$$[G]: \sum_{p=1}^{N} M_p \times N \tag{6}$$

So far, this version of the moment method has been used assuming $M_p = 1$ for each p. Since this approach constrains the solution only at the central points of the cells [14], [17], the overconstrained moment method could better constrain the solution to the scatterer's geometric shape and dielectric discontinuities. In particular, we assume M_p to be larger than 1 in the cells near edges and corners, where strong variations may occur in the electromagnetic field. In this way, while we can still approximate the field value inside a cell by a constant value, we can also constrain such a value to be the one that best fits not only the field value at the cell center but also the field values at all testing points in the cell. Of course, when we adopt the proposed approach assuming $M_p > 0$ in some cells, the Green matrix $[G]$ turns out to be a rectangular matrix, hence a solution to system (2) cannot in general be reached in a classical way. However, a least-squares pseudosolution to system (2) can be obtained by applying a pseudoinversion algorithm [15], [16].

The use of a large number of testing functions would result in higher computational accuracy, though by use of the same number of basis functions. While, for traditional MoM, the only proper action for the field evaluation in regions where the e.m. field varies to an appreciable amount is to increase the discretization cells number, the overconstrained MoM could yield equal simulation results considering a reduced number of cells. The examples given in the following show that this goal can be attained, provided that the number of testing points and their locations are correctly selected.

III. Numerical Results and Discussion

Here we present the results obtained by the algorithm described in the preceding section. In order to test the validity of the approach, we focused our attention on three cases previously reported in the literature [14], as they had been considered to evaluate the convergence and accuracy of the traditional MoM version.

The assumed configuration is a homogeneous dielectric cube (edge length: "L"), illuminated by a uniform plane wave propagating in the z direction and polarized with the electric field vector along the x axis (Fig. 1).

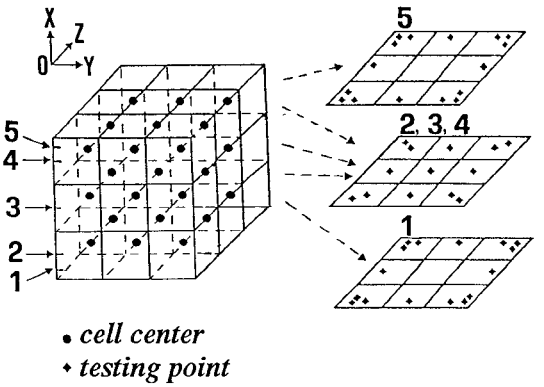

Fig. 1. Schematic representation of the scattering geometry and testing-point locations for a 27-cell model.

In the first set of simulations, we considered an edge length of 0.5 cm and the following dielectric parameters: $\varepsilon_r = 77.1$ and $\sigma = 1.40$ S/m. The operating frequency was 400 MHz and the average power density was equal to 1 mW/cm^2 [14]. More than one point for each cell was assumed for the cells near corners and edges (for inhomogeneous objects, redundant testing points should be located near discontinuities). In particular, in each cell near a corner, testing points were placed on the segments linking the cell center to the corner and the cell center to the middle points of the three segments forming the corner. Another testing point was placed at the center of each cell. In each cell near an edge, testing points were located at the cell center and on the segment linking the cell center to the middle point of the edge. A global view of the testing points for a 27-cell model is shown in Fig. 1. For this discretization, we located only one testing point on each of the previously defined segments; as a result, we had $M_p = 5$ in the corner cells and $M_p = 2$ in the edge cells, for a total of 71 testing points. To fix the location of each testing point on the related segment, we used the following rule: we call an "hth configuration" the configuration of testing points in the case where the distance between each testing point (on the related segment) and the cell center is equal to hl/n (l being the length of the related segment and n being a fixed number that is equal for all testing points).

For these examples,we assumed $n = 25$, giving 24 possible different configurations ($h = 1, \cdots, 24$). The results of the numerical simulations were obtained by using the above values. Fig. 2 shows the histogram of the percent errors on the evaluations of the average Specific Absorption Rate (SAR) for the 24 configurations, defined as

$$\mathrm{ERR} = \frac{|\mathrm{SAR} - \mathrm{SAR}_{\mathrm{convergence}}|}{|\mathrm{SAR}_{\mathrm{convergence}}|} \times 100. \tag{7}$$

Such errors were evaluated taking, as a convergence value, the extrapolated value reported in [14]. As the errors depend on the positions of the testing points, then great care must be exercised in selecting such positions. However, the histogram shows that an area exists for which the error is very small, hence the SAR can be estimated to an accuracy that is

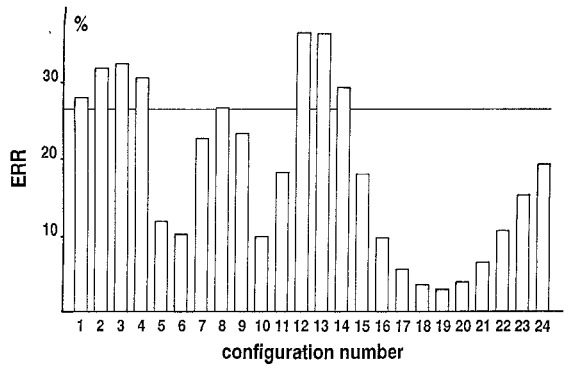

Fig. 2. Percent errors on the evaluations of the average SAR versus the 24 different positions of the testing points for the first simulation ($\varepsilon_r = 77.1, \sigma = 1.40$ S/m, edge length = 0.5 cm). Continuous line: 27-cell traditional MoM.

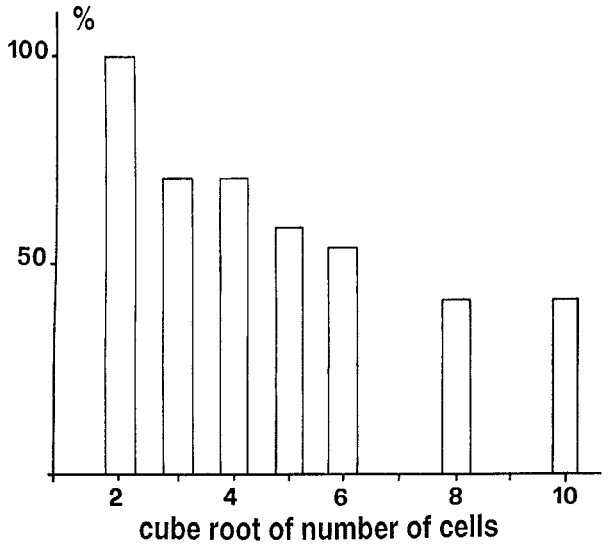

Fig. 3. Percentage of 27-cell overconstrained cases giving SAR values better than those obtained by classical MoM implementations for various discretizations. First simulation case ($\varepsilon_r = 77.1, \sigma = 1.40$ S/m, edge length = 0.5 cm).

comparable to that reached by a classic MoM using 64 or more cells.

Fig. 3 shows the percentage of 27-cell overconstrained cases that gave better estimates of the average SAR than "classic cases" using various discretizations. As can be seen, over 50 percent of the simulations yielded average SAR values comparable to (or better than) those given by a 64-cell traditional MoM.

For this first example, another set of simulations were performed, using a 64-cell discretization. We used $M_p = 5$ for the corner cells and $M_p = 2$ for the edge cells, for a total of 120 testing points. In Fig. 4, the SAR behavior is presented and compared with those obtained in "classical" MoM cases considering 125 and 216 cells. It can be seen that the use of 64 cells results in a more regular behavior of the SAR values, which, for any configuration, is close to the convergence value. The same figure also shows the plots related to 1- and 8-cell OMoMs; these plots were obtained by following the previously described rule for choosing corner and edge testing points.

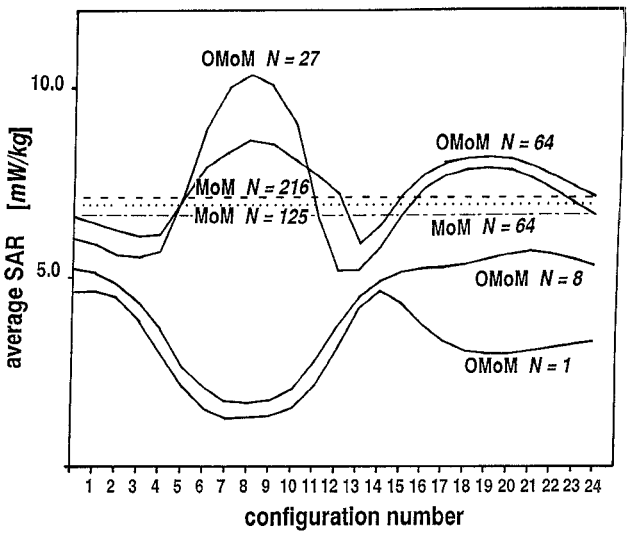

Fig. 4. First set of simulations ($\varepsilon_r = 77.1, \sigma = 1.40$ S/m, edge length = 0.5 cm): average SAR's in overconstrained cases for 1-, 8-, 27- and 64-cell discretizations. The numbers of the 24 configurations are given on the abscissa. The same figure also presents the average SAR values obtained by a 64-cell, a 125-cell, and a 216-cell traditional MoM.

These cases, however, are far from convergence, hence very good simulation results cannot be expected.

The second set of simulations were performed considering a cube with an edge length of 2.5 cm and the dielectric parameters $\varepsilon_r = 77.1$ and $\sigma = 1.40$ S/m; the cube was illuminated by a plane wave at a frequency of 400 MHz [14]. A 27-cell discretization was used. In this case, the convergence value was not available, so we used another parameter for comparison purposes. As the average SAR value increases monotonically with the cube subdivision [14], it was interesting to deduce the improvement in SAR evaluation (obtained by the overconstrained method) from the increases in the various SAR values. Fig. 5 presents the SAR behavior versus the locations of the testing points, for a 27-cell discretization, and Fig. 6 shows the percentage of 27-cell overconstrained cases giving better SAR values than those obtained by classical MoM implementations for various discretizations. Even in the case of a 2.5-edged cube, it appears that the overconstrained MoM may lead to an improvement in the solution. It is worth noting that it is easy to make a suitable choice of testing points: for over 60 percent of the simulations, the OMoM gave SAR values that were better than the values given by a classic 64-cell MoM scheme.

The third set of simulations dealt with a cube with an edge length of 30 cm and the dielectric parameters $\varepsilon_r = 76.0$ and $\sigma = 0.42$ S/m; the cube was illuminated by a plane wave at a frequency of 27.12 MHz. This simulation arrangement was previously considered by many authors [7], [14]. Evenin this case, an improvement over a classic MoM solution was achieved, as shown in Figs. 7 and 8.

In particular, it should be noted that, in all the cases considered, a region between the center of a cell and an edge or corner exists for which a certain improvement can be expected, and for which the positions of the testing points are not too critical. Although, at the present stage of our

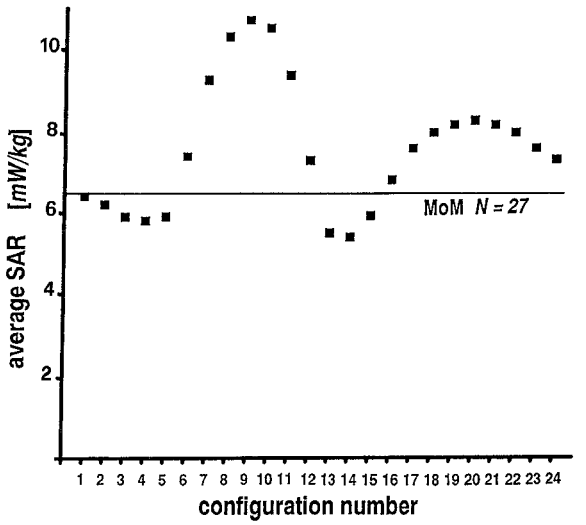

Fig. 5. Behavior of the average SAR versus the locations of the testing points, for a 27-cell discretization, in the second simulation case ($\varepsilon_r = 77.1, \sigma = 1.40$ S/m, edge length = 2.5 cm).

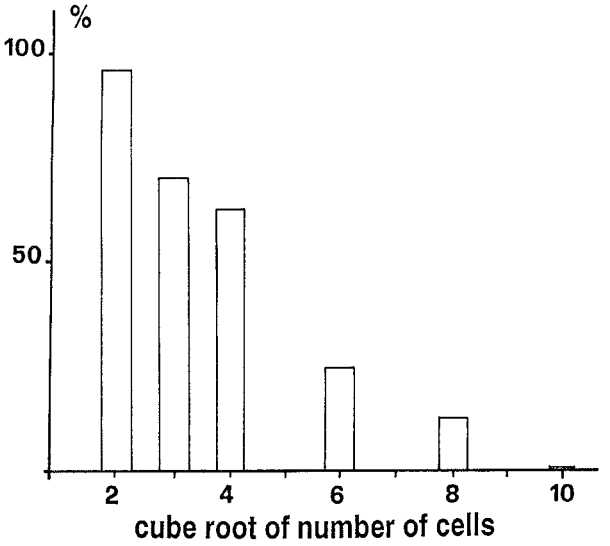

Fig. 6. Percentage of 27-cell overconstrained cases giving SAR values larger than those obtained by classical MoM implementations for various discretizations. Second simulation case ($\varepsilon_r = 77.1, \sigma = 1.40$ S/m, edge length = 2.5 cm)

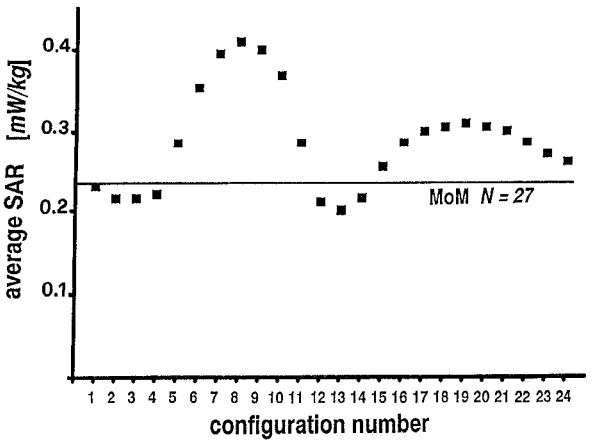

Fig. 7. Behavior of the average SAR versus the location of the testing points, for a 27-cell discretization, in the third simulation case ($\varepsilon_r = 76.0, \sigma = 0.42$ S/m, edge length = 30 cm).

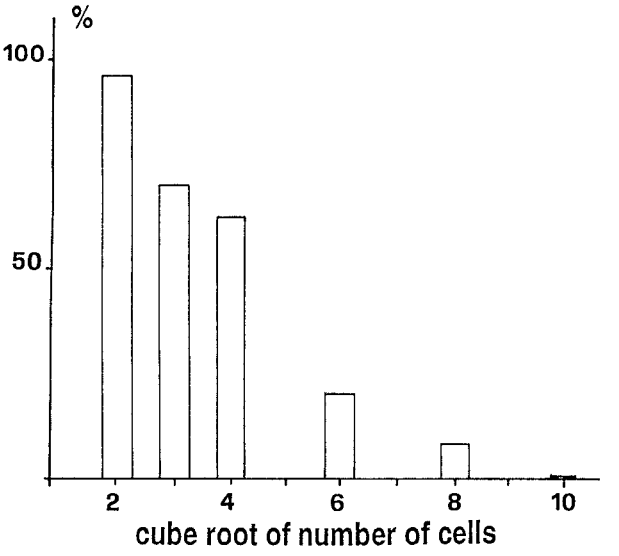

Fig. 8. Percentage of 27-cell overconstrained cases giving SAR values larger than those obtained by classical MoM implementations for various discretization. Third simulation case ($\varepsilon_r = 76.0, \sigma = 0.42$ S/m, edge length = 30 cm).

research, rigorous criteria for selecting the testing points are not available, a rule-of-the-thumb for a suitable choice of the overconstraining testing points could be deduced from the results of the numerical simulations performed. For instance, one might use the following criterion: according to the rule for locating the testing points on given segments (described at the beginning of the Section), an "hth configuration" must be chosen, with h ranging between the limits:

$$\lceil \tfrac{2}{3}n \rceil \leq h \leq \lceil \tfrac{4}{5}n \rceil + 1 \tag{8}$$

where n is a fixed number (equal for all testing points), as defined at the beginning of Section III, and the symbol "$\lceil \xi \rceil$" stands for the integer part of ξ.

This rule may lead to an error on SAR evaluation that is about 60% smaller than the one obtained by the classical MoM solution for the same discretization.

Finally, to allow an evaluation of the cost/benefits ratio related to the proposed method, in terms of computational load, Table I gives the CPU times and the memory units for the Green matrix (i.e., the element that requires most of the memory), for some of the configurations considered. Note that each additional testing point introduces an overhead into the dimensions of the Green matrix, as compared with the classical MoM. Nevertheless, this overhead is very limited, in that the dimensions of the Green matrix increase linearly with the number of testing points, while the addition of a cell would involve a quadratic increment. All the values have been normalized to the ones related to the 27-cell traditional MoM. It is interesting to note that the use of an OMoM with only 27 cells but 71 testing points requires computational

TABLE I
HOMOGENEOUS DIELECTRIC CUBE: CPU TIMES AND MEMORY REQUIRED FOR THE GREEN MATRIX. ALL VALUES HAVE BEEN NORMALIZED TO THE ONES RELATED TO THE 27-CELL TRADITIONAL MoM.

	CPU time units	Memory units
MoM 27	1.00	1.00
OMoM 27 (71 testing points)	2.35	2.63
MoM 64	5.39	5.62
OMoM 64 (120 testing points)	19.68	10.53
MoM 125	33.17	21.43
MoM 216	144.23	64.00

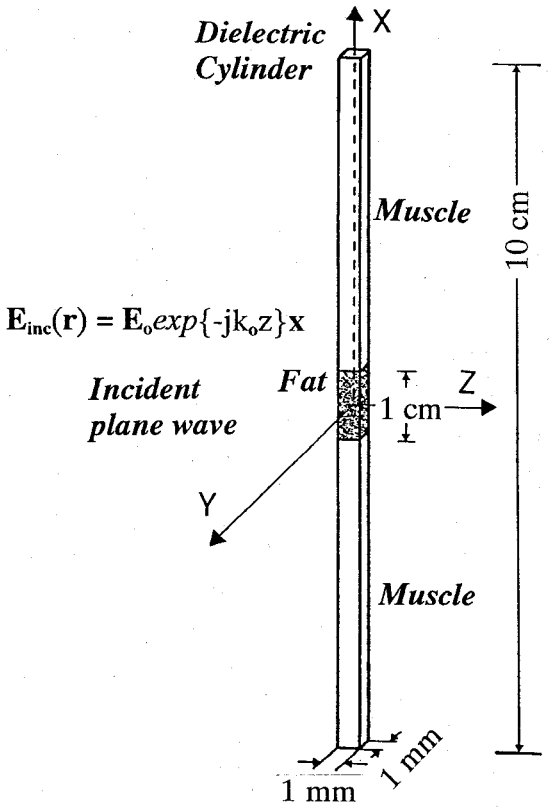

Fig. 9. Geometry of the inhomogeneous scatterer (fat: $\varepsilon_r = 4.7$ and $\sigma = 0.15$ S/m; muscle: $\varepsilon_r = 48.4$ and $\sigma = 2.1$ S/m).

resources that are fewer than half the ones necessary for a 64-cell classical MoM, whereas the obtained results can be compared with those of a traditional MoM using 124-cells or more cells. Therefore the 27-cell OMoM needs a limited computational overhead to yield a notable improvement over the classical MoM solution.

We also wanted to assess the capability of the OMoM in the case of a dielectric discontinuity. To this end, we considered a cylinder of finite length (10 cm), made of fat ($\varepsilon_r = 4.7$ and $\sigma = 0.15$ S/m) and muscle ($\varepsilon_r = 48.4$ and $\sigma = 2.1$ S/m) (as in the work by Livesay and Chen [2]) and illuminated by a plane wave at a frequency of 2.45 GHz. Fig. 9 shows the geometry considered. Such a geometry causes the total electric field to be mainly parallel to the cylinder axis; so it is easy to evaluate the behavior of the method of considering only one field component. The cylinder was subdivided into 100 cubical cells of equal size (1-mm edge).

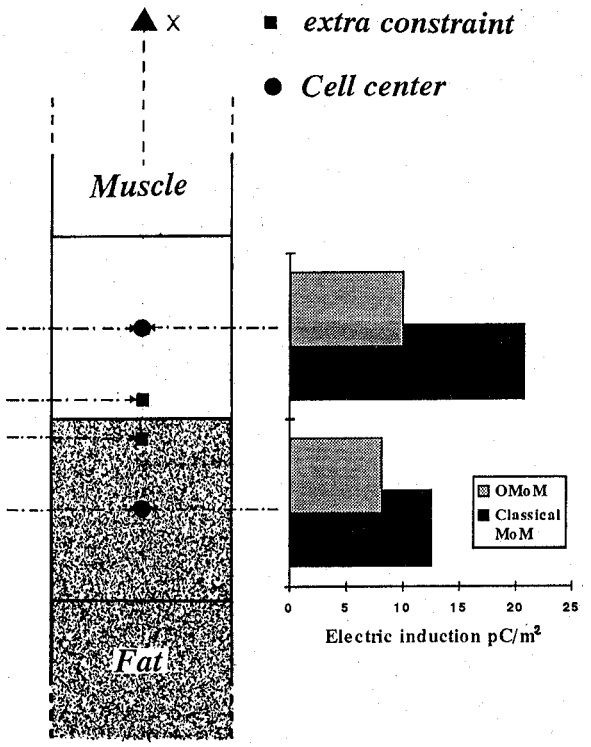

Fig. 10. Testing-point locations near a fat-muscle interface, and histogram of the amplitude of the x component of the electric displacement vector $\boldsymbol{D}$ [C/m^2] near the interface.

We enforced the constraints on each discontinuity region between muscle and fat in order to satisfy (even though in an approximate way) the continuity condition on the normal component of the electric displacement vector $\boldsymbol{D}$. To this end, we used 2 testing points in each cell at the interfaces, for a total of 104 testing points. Fig. 10 points out that the results obtained by the classical MoM are affected by large discontinuities near the interfaces. The OMoM solution, on the contrary, seems much more regular. Note that the classical MoM solution was absolutely insufficient to ensure the continuity of $\boldsymbol{D}$ across the interfaces, as the electric-displacement amplitude in muscle is 1.7 times that in fat. Instead, the OMoM gave very close values, the ratio between the two amplitude values being equal to 1.1.

IV. CONCLUSIONS

A numerical method has been analyzed in applications to scattering problems inside bodies whose features resembled those of biological tissues. The method is an overconstrained version of the traditional MoM, and allows one to take into account the strong field variations occurring on the edges and in the corners of a scatterer. It has been shown that the method may sensibly enhance the convergence of the solution, thus allowing a considerable saving in computer resources. At the present stage, the method requires some care in choosing the best locations for the overconstraints; only a rule-of-the-thumb has been derived for the best choice of additional testing points. Future work will be aimed at studying realistic models of biological bodies by using the OMoM. Such models will definitively demonstrate the capabilities and limitations of the

proposed approach. Moreover, the method may be further refined by using more suitable testing functions to smooth away the field variations that may result from changing the positions of edge and corner testing points.

REFERENCES

[1] R. F. Harrington, *Field Computation by Moment Method.* New York: Macmillan, 1968.

[2] D. E. Livesay and Kun-Mu Chen, "Electromagnetic fields induced inside arbitrarily shaped biological bodies," *IEEE Trans. Microwave Theory Tech.*, vol. MTT-22, pp. 1273–1280, 1974.

[3] J. F. Deford, O. P. Gandhi, and M. J. Hagmann, "Moment-method solutions and SAR calculations for inhomogeneous models of man with large number of cells," *IEEE Trans. Microwave Theory Tech.*, vol. MTT-31, pp. 848–851, 1983.

[4] K. D. Paulsen, D. T. Lynch, and J. W. Strohbehn, "Three-dimensional finite, boundary, and hybrid element solution of the Maxwell equations for lossy dielectric media," *IEEE Trans. Microwave Theory Tech.*, vol. 36, pp. 682–693, 1988.

[5] D. M. Sullivan, D. T. Borup, and O. P. Gandhi, "Use of the finite-differences time-domain method in calculating EM absorption in human tissues," *IEEE Trans. Biomed. Eng.*, vol. BME-34, pp. 148–157, 1987.

[6] D. M. Sullivan, O. P. Gandhi, and A. Taflove, "Use of the finite-difference time-domain method for calculating EM absorption in man models," *IEEE Trans. Biomed. Eng.*, vol. 35, pp. 179–186, 1988.

[7] H. Massoudi, C. H. Durney, and M. F. Iskander, "Limitations of the cubical block model of man in calculating SAR distributions," *IEEE Trans. Microwave Theory Tech.*, vol. MTT-32, pp. 746–752, 1984.

[8] M. J. Hagmann and R. L. Levin, "Criteria for accurate usage of block models," *J. Microwave Power*, pp. 19–27, 1987.

[9] M. J. Hagmann and R. L. Levin, "Accuracy of block models for evaluation of the deposition of energy by electromagnetic fields," *IEEE Trans. Microwave Theory Tech.*, vol. MTT-34, pp. 653–659, 1986.

[10] D. H. Schaubert, D. R. Wilton, and A. W. Glisson, "A tetrahedral modeling method for electromagnetic scattering by arbitrarily shaped inhomogeneous dielectric bodies," *IEEE Trans. Antennas Propagat.*, vol. AP-32, pp. 77–85, 1984.

[11] C.-T. Tsai, H. Massoudi, C. H. Durney, and M. F. Iskander, "A procedure for calculating fields inside arbitrarily shaped, inhomogeneous dielectric bodies using linear basis functions with the moment method," *IEEE Trans. Microwave Theory Tech.*, vol. MTT-34, pp. 1131–1139, 1986.

[12] T. K. Sarkar, "A note on the choice of weighting functions in the method of moments," *IEEE Trans. Antennas Propagat.*, vol. AP-33, pp. 436–441, 1985.

[13] S. Caorsi, G. L. Gragnani, and M. Pastorino, "Overconstrained version of moment method for prediction of electromagnetic energy deposition inside dielectric objects," *Elec. Lett.*, vol. 26, pp. 1997–1998, 1990.

[14] M. J. Hagmann and R. L. Levin, "Convergence of local and average values in three-dimensional moment-method solutions," *IEEE Trans. Microwave Theory Tech.*, vol. MTT-33, pp. 649–654, 1985.

[15] M. M. Ney, "Method of moments as applied to electromagnetic problems," *IEEE Trans. Microwave Theory Tech.*, vol. MTT-33, pp. 972–980, 1985.

[16] B. Rust, W. R. Burrus, and C. Schneeberger, "A simple algorithm for computing the generalized inverse of a matrix," *Comm. ACM*, vol. 9, pp. 381–387, 1966.

[17] B. S. Guru and K. M. Chen, "Experimental and theoretical studies on electromagnetic fields induced inside finite biological bodies," *IEEE Trans. Microwave Theory Tech.*, vol. MTT-24, pp. 433–440, 1976.

Salvatore Caorsi received the "laurea" degree in electronic engineering from the University of Genoa, Genoa, Italy, in 1973.

After graduation he remained at the university as a researcher, and since 1976 he has been Professor of Antennas and Propagation. In 1983 he also assumed the title of Professor of Fundamentals of Remote Sensing. He is presently with the Department of Biophysical and Electronic Engineering where he is responsible for the Applied Electromagnetics Group and for the Research Center on the Interaction Between Electromagnetic Fields and Biological Systems (IEMBS). His primary activities are focused on applications of electromagnetic fields to telecommunications, artificial vision and remote sensing, biology, and medicine. In particular, he is working on research projects concerning microwave hyperthermia and radiometry in oncological therapy; numerical methods for solving electromagnetic problems; and inverse scattering and microwave imaging.

Mr. Caorsi is a member of the Associazione Elettrotecnica ed Elettronica Italiana (AEI), of the European Bioelectromagnetism Association (EBEA) and of the European Society for Hyperthermic Oncology (ESHO).

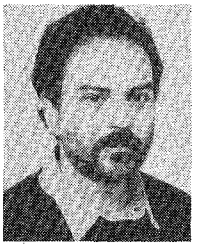

Gian Luigi Gragnani (M'89) received the "laurea" degree in electronic engineering from the University of Genoa, Genoa, Italy, in 1985.

In the same year, he joined the Applied Electromagnetics Group in the Department of Biophysical and Electronic Engineering. His primary research interests are in the field of electromagnetic scattering (both direct and inverse). In particular, he is engaged in doing research work on numerical methods for addressing electromagnetic problems, on microwave imaging, on biomedical applications of electromagnetic fields (especially microwave hyperthermia), and on electromagnetic compatibility.

Mr. Gragnani is a member of the Associazione Elettrotecnica ed Elettronica Italiana (AEI), and of the European Bioelectromagnetism Association (EBEA).

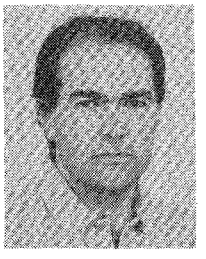

Matteo Pastorino (M'90) received the "laurea" degree in electronic engineering from the University of Genoa, Genoa, Italy, in 1987 and the Ph.D. degree in electronics and computer science from the same university in 1992.

Since that year, he has cooperated on the activities of the Applied Electromagnetics Group and of the Research Center on the Interaction Between Electromagnetic Fields and Biological Systems. At present he is a researcher of Electromagnetic Fields in the Department of Biophysical and Electronic Engineering. His main research interests are in electromagnetic direct and inverse scattering, microwave imaging, wave propagation in presence of nonlinear media, and in numerical methods in electromagnetism. He is also working on research projects concerning biomedical applications of e.m. fields and microwave hyperthermia.

Dr. Pastorino is a member of the Associazione Elettrotecnica ed Elettronica Italiana (AEI), and of the European Bioelectromagnetism Association (EBEA).